



*Supplement of*

## **Derivation of bedrock topography measurement requirements for the reduction of uncertainty in ice-sheet model projections of Thwaites Glacier**

**Blake A. Castleman et al.**

*Correspondence to:* Blake A. Castleman (bcastleman3@gatech.edu)

The copyright of individual parts of the supplement might differ from the article licence.

## Supplementary

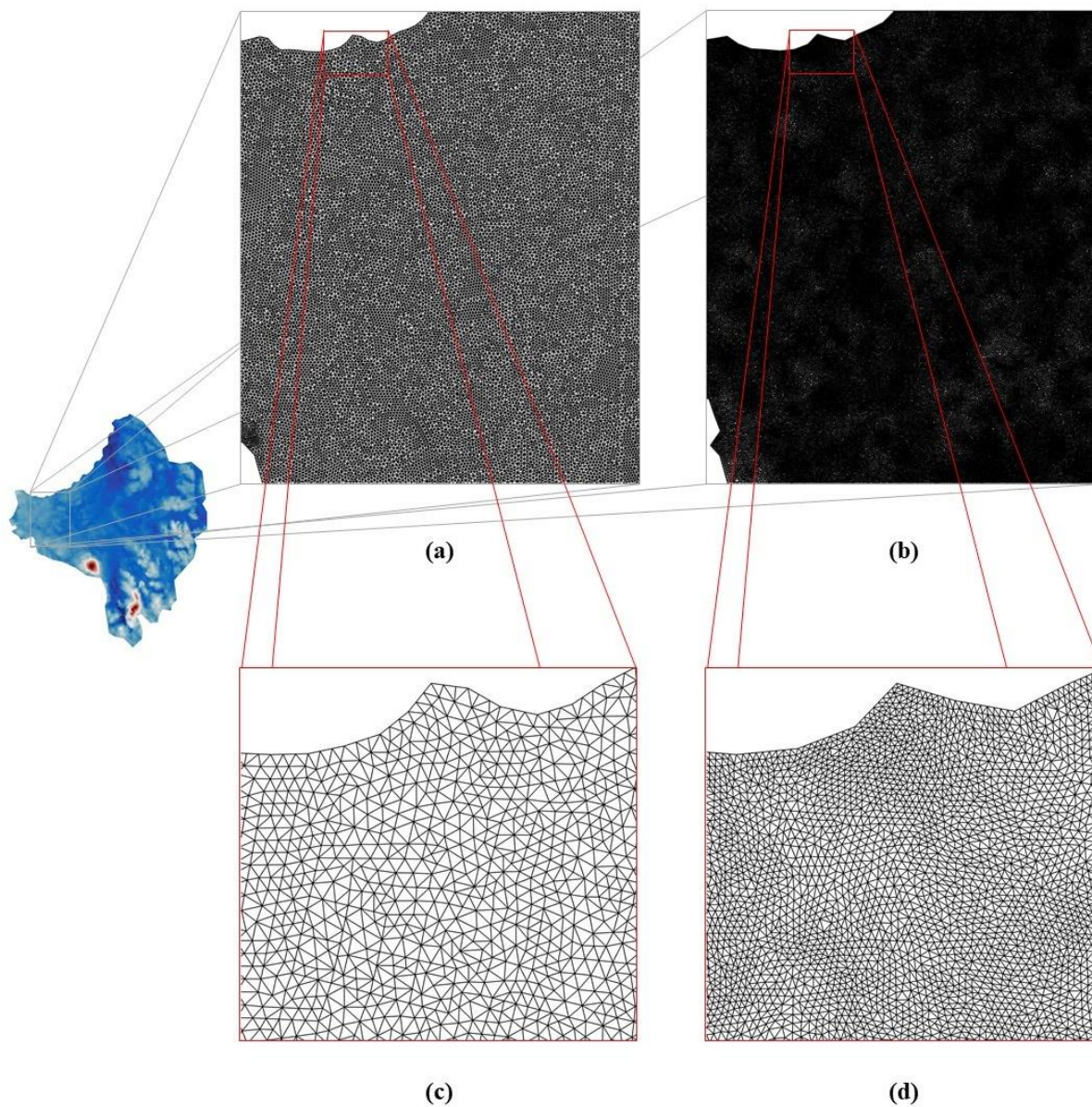


**Fig. S1:** The meshes defined for (a) vertical tests and (b) spatial tests are compared side by side in one of the regions closest to the initial grounding line. A further zoom allows visual observation of element size differences (c, vertical test mesh; d,

spatial test mesh).

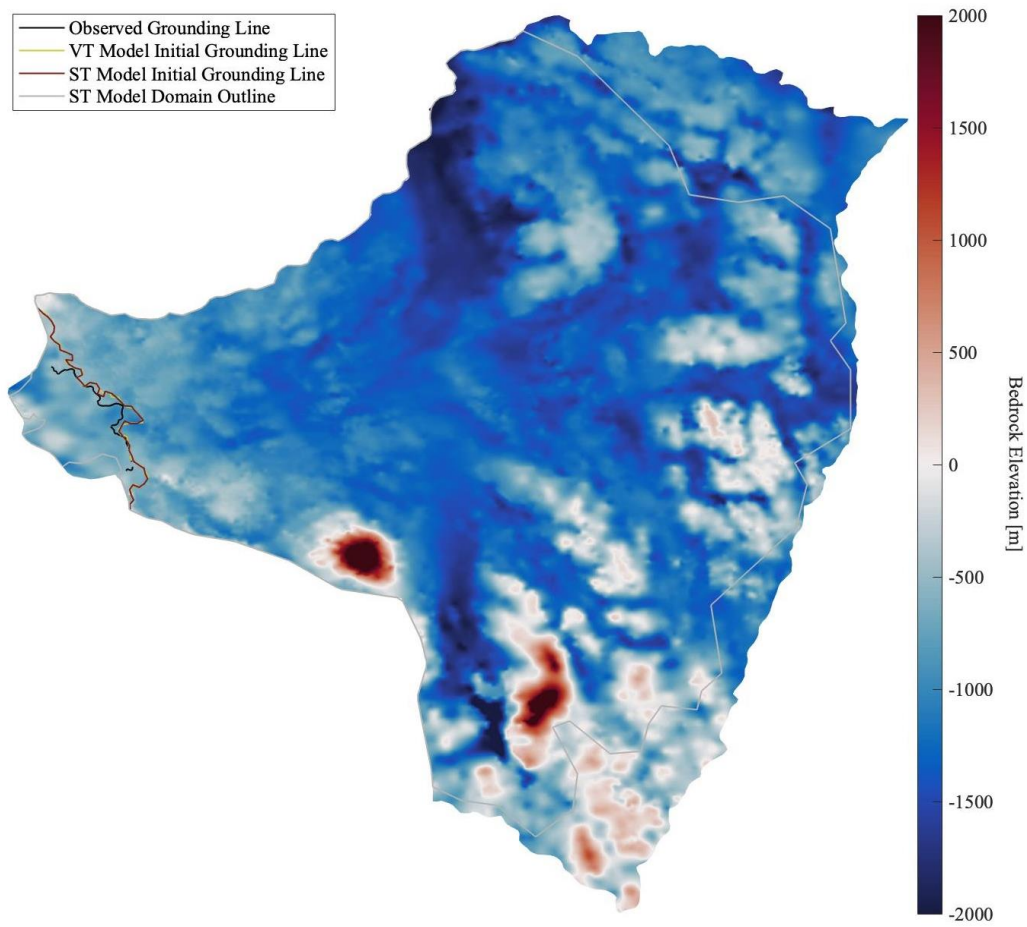
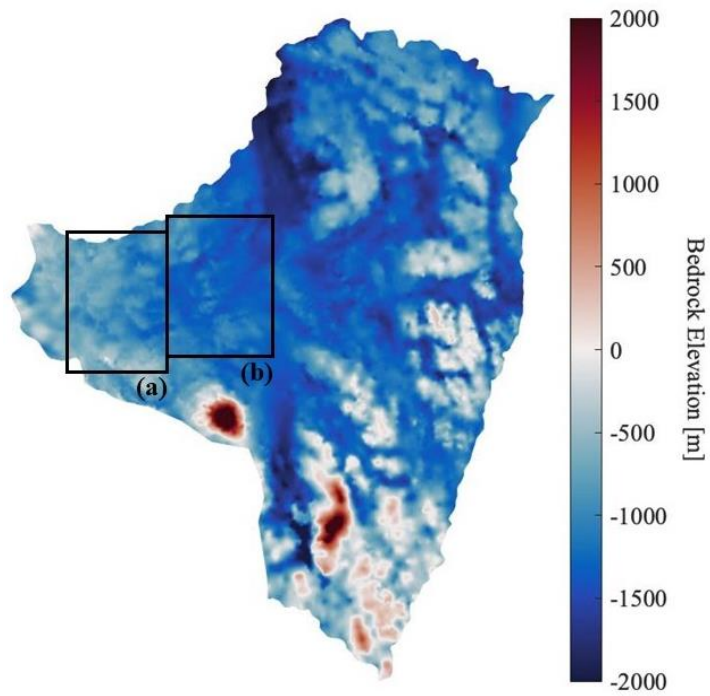


**Fig. S2:** Initial grounding line comparison between the observed grounding line in Yu et al (2018; gray), the VT model (yellow), and the ST model (red). The VT and ST models are closely aligned and are started slightly ahead of the observed grounding line. The domain outline used in the spatial model (white) is also portrayed for comparison against the vertical model (plot domain).



15

**Fig. S3:** The two primary sets of ridges that we detail are depicted. Set **(a)** borders the grounding line and contains the largest pinning features while set **(b)** is a thinner, more sparse collection.

20

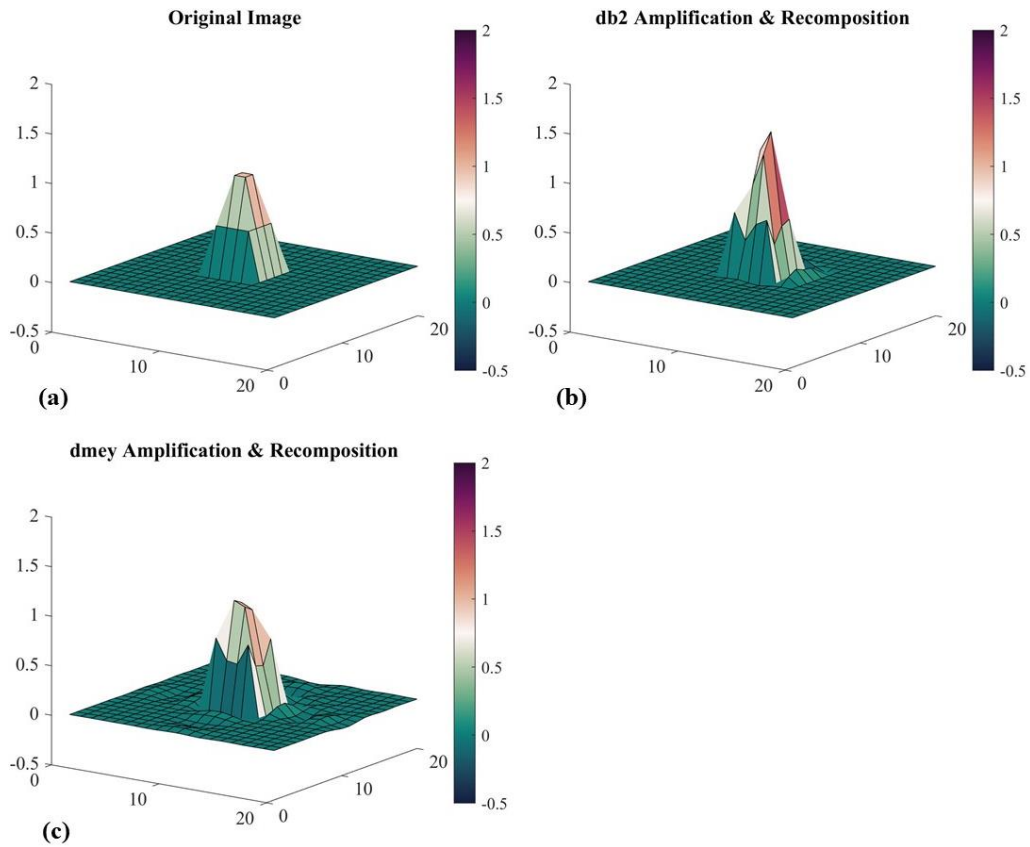


**Fig. S4:** (a) An ordinary peak is decomposed, amplified, and recomposed with the (b) db2 and (c) dmey wavelets. Amplification occurs at 100% on the first resolution level for both wavelets. The (b) db2 recomposition exhibits sharper and higher amplitude peaks as compared to the (c) dmey recomposition, which exhibits smoother, wave-like characteristics.

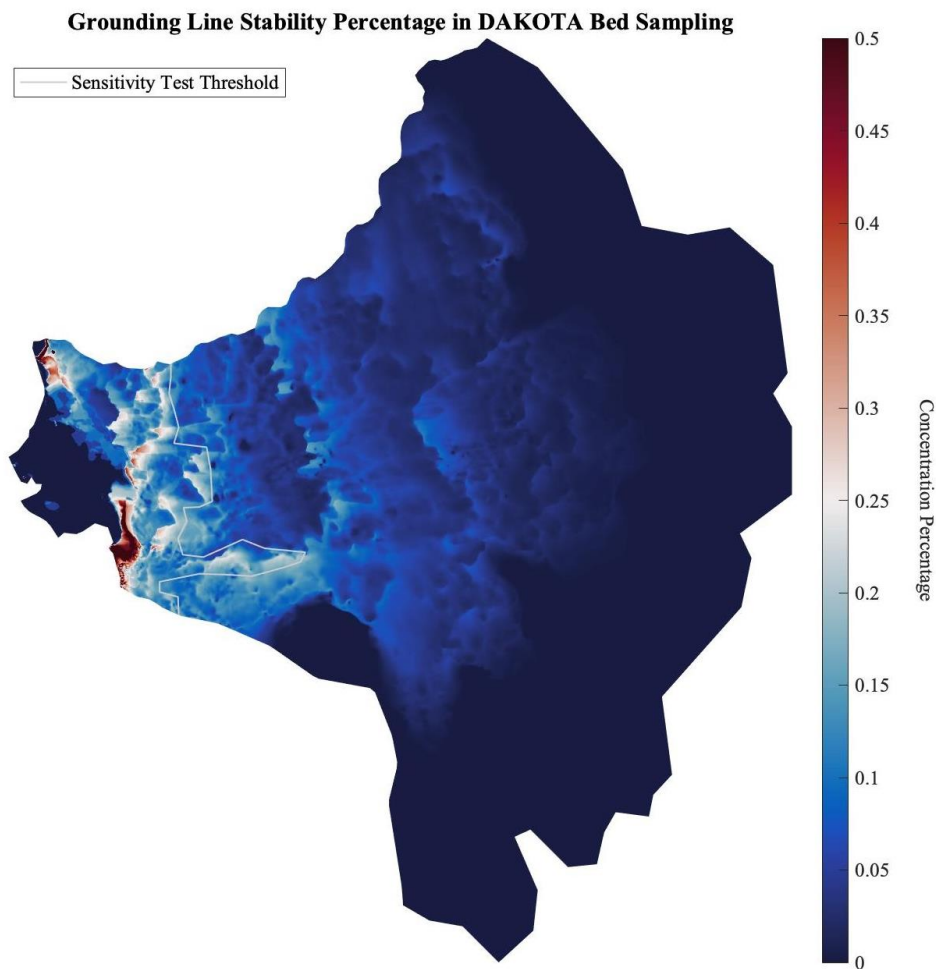


**Fig. S5:** The probability of the grounding line's location lying on an element during a 200-year projection forced with extreme (1.8 times present day) ice shelf basal melting rates, as determined from random sampling of bedrock topography within a prescribed 3% error (described in Sect. 5.1 and portrayed in Fig. 5, blue line). Grounding line positions are calculated every 10 years for all of the 300 forward simulations in the ensemble, resulting in 6000 different grounding line configurations. Plotted is the concentration of all 6000 grounding line positions as a percentage of the amount of times the grounding line is located in an individual location. A threshold line (gray) is drawn to segregate the percentages at or above 20%. This figure is the determining factor for analyzing and testing relevant regions in our sensitivity test (Sect. 5.2).



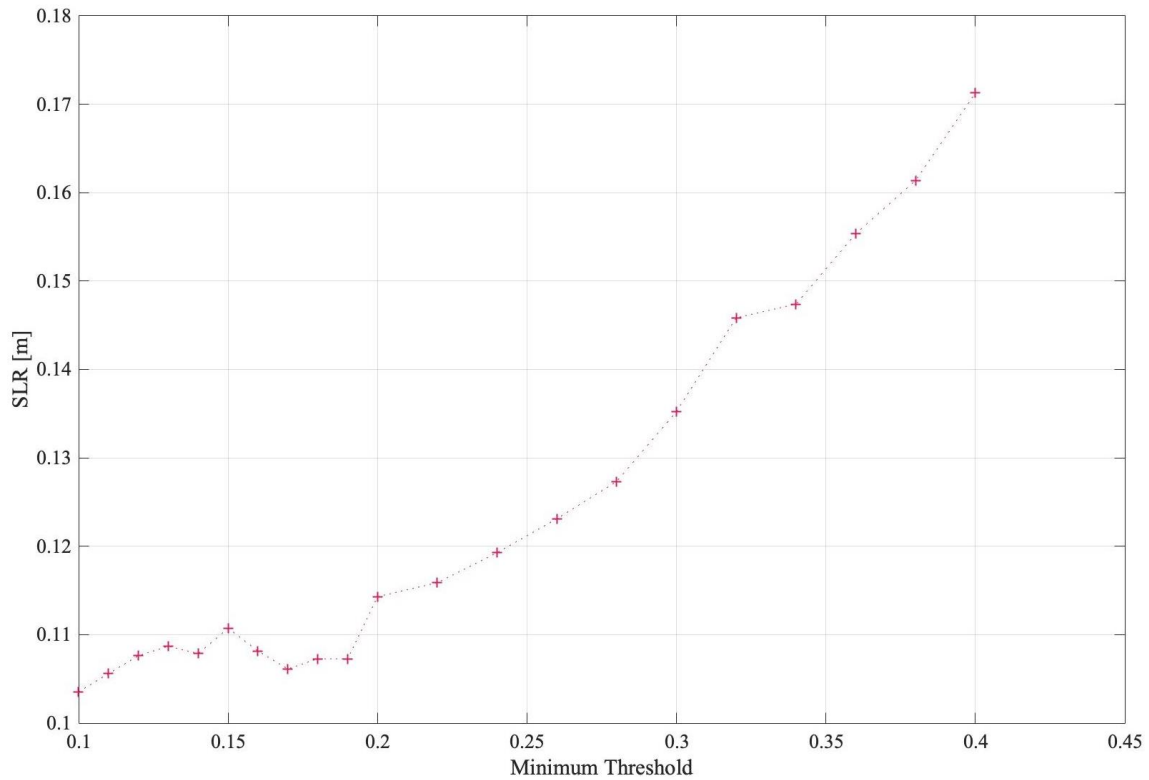
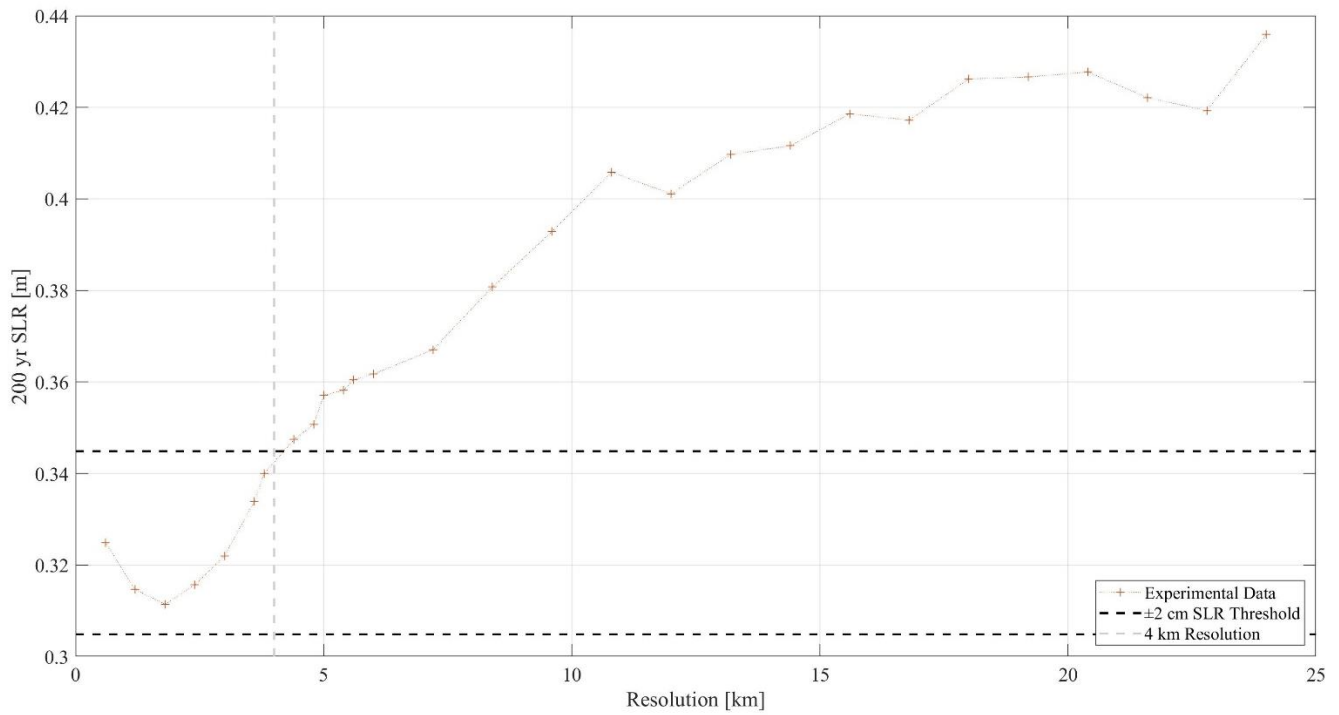


**Fig. S6:** SLR contribution as a function of positive perturbations in bedrock topography. Perturbations are only made at points that fall above a minimum threshold of grounding line concentration probability derived from the bedrock sampling  $\times 1.8$  melt ensemble (Fig. S4). We use this figure to determine what grounding line concentrations we should set our limits to when deciding what regions of bedrock topography in Fig. S4 are most relevant to investigate as significant pinning points. In this case, we determine that 20% is an appropriate threshold.



45 **Fig. S7:** Experiment 2 (Sec. 4.2) is repeated with a  $\times 3.6$  basal melt multiplier. The decomposition occurs with the db2 wavelet to the first resolution level ( $n = 1$ ) with a 10,000% high frequency matrix amplification (denoted as “Wvlt: db2 | Lvl: 1 | %: 10000” by Sec. 9.2). The new spatial resolution threshold for this trial is observed to decrease to 4 km.

50